Schiff Base and their Mn (II), Ni (II), Co (II), Zn (II), Cu (II), Pt (II) and Pd (II) Complexes, Spectral studies with Anti-Microbial Activity

Priyanka S Thakur and Manohar V. Lokhande *
Department of Chemistry, Sathaye College (Autonomous), Mumbai – 400057, Maharashtra, India.

***Abstract*— A variety of transition metal ion complexes have been synthesized due to their significant analytical and commercial importance. Complexes of the general formula [ML·2H₂O], where [M = Mn(II), Ni(II), Co(II), Cu(II), Pt(II), Pd(II) and Zn(II), and L=(E)-2-[(6-chloropyridin-2-yl) iminomethyl] naphthalen-1-ol] have been successfully prepared and characterized. The characterization was carried out using elemental analysis, FTIR, UV–Visible, TGA/ DTA mass spectrometry, magnetic susceptibility, antimicrobial studies and conductivity measurements, The complexes exhibit a metal-to-ligand ratio of 1:1 with Ni (II) Complexes has octahedral geometry. Magnetic susceptibility data, along with electronic spectra results, suggest that the complexes possess a Octahedral geometry. Infrared spectral analysis of both the ligand and the complexes confirm coordination through the nitrogen atom and Oxygen atom of Hydroxy group to the central metal ion. Additionally, bonding parameters (b½) and the nephelauxetic ratio (β) were evaluated using electronic spectral data. Conductivity measurements indicate that the complexes behave as non-electrolytic in nature. Furthermore, antimicrobial activity studies show that both the ligand and its complexes exhibit enhanced activity against Gram-positive and Gram-negative microorganisms.**

Key words: **Antimicrobial studies, FTIR, Mass spectrometry, magnetic susceptibility TGA/ DTA , and UV–Visible**

I. INTRODUCTION

Over the past decade, considerable attention has been devoted to the coordination chemistry of transition elements due to their wide-ranging applications [1-2]. These include their use as probes in medicinal and biological systems, as contrast agents in magnetic resonance imaging, and as mild reagents and catalysts in organic synthesis [3-4]. Schiff bases represent a significant category of ligands in coordination chemistry, widely recognized for their ability to coordinate with metal ions through various donor atoms. Their versatility in forming stable complexes has been extensively documented in the literature [5-6]. Transition metal complexes derived from Schiff bases continue to attract considerable attention due to their diverse structural characteristics and notable biological activities [7-8].

Moreover, these coordination compounds have been thoroughly studied because they exhibit unique structural arrangements, interesting magnetic behavior, and play an important role in various biological processes [9-10]. Schiff base complexes are widely studied for their versatile applications, particularly in antimicrobial activity [11], catalysis [12], and material science [13]. Transition metal complexes of Schiff bases show enhanced biological activity compared to free ligands, making them promising candidates in medicinal and industrial chemistry. Such applications demand a thorough understanding of the coordination behavior of transition metal ions [14]. In particular, complexes containing macrocyclic ligands with hard donor atoms have been extensively investigated. This has inspired the present study on transition metal complexes with the ligand =(E)-2-[(6-chloropyridin-2-yl) iminomethyl] naphthalen-1-ol].

II. MATERIAL AND METHODOLOGY

Material: All chemicals used in this study were of analytical reagent (AR) grade, while some were of BDH grade. 2-Hydroxynaphthalene-1-carbaldehyde and 6-chloropyridine-2,4-diamine obtained from Sigma Aldrich The metal salts employed included $MnCl_2$, $NiCl_2·6H_2O$, $CoCl_2·6H_2O$, $CuCl_2·2H_2O$, Pt(II), Pd(II) and $ZnCl_2$. Solvents such as methanol, ethanol, chloroform, and water were purified by double distillation before use.

Methodology: The carbon, hydrogen, and nitrogen contents of the ligand and its complexes were determined using microanalytical techniques at IIT Mumbai. Infrared (FTIR) spectra of the ligand and corresponding complexes were recorded using KBr pellet methods on a PerkinElmer spectrophotometer. Chloride content was estimated by Mohr's method., while electronic spectra were recorded at UICT Mumbai using DMSO and water as solvents. Thermogravimetric analysis (TGA) and differential thermal analysis (DTA) were performed on a Mettler Toledo Star system over a temperature range of 20–850 °C. Mass spectra were recorded using the ESI technique at IPCA Laboratories. The melting point of the ligand and decomposition temperatures of the complexes were determined. Molar conductance measurements (10^{-3} M) were carried out in DMSO and water using a digital conductivity meter calibrated with KCl solution. Magnetic susceptibilities of the complexes were determined using a Gouy balance, with Hg $[Co(SCN)_4]$ employed as the calibrant.

Preparation of the Ligand: Equimolar amounts (0.2 mol each) of 2-Hydroxynaphthalene-1-carbaldehyde and 6-chloropyridine-2,4-diamine were dissolved in ethanol. To this solution, 3 cm³ of acetic acid was added, and the reaction mixture was refluxed for three hours using a water condenser. Upon completion of the reaction, a solid product separated out. The precipitate was cooled, filtered, washed with ethanol, and dried at room temperature, followed by further drying at 60°C to obtain the final ligand.

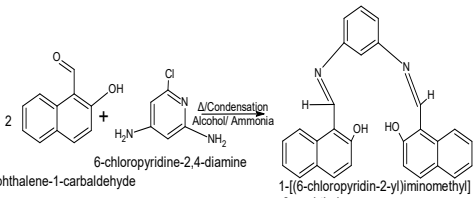

Preparation of the Complexes: Solutions of metal chlorides (0.01 M) and the ligand were prepared in ethanol. These solutions were mixed in a 1:1 metal-to-ligand stoichiometric ratio. The ligand solution was added slowly to an acidic aqueous solution of the metal salt with continuous stirring. The pH of the resulting mixture was adjusted to approximately 5.8–6.3 by the gradual addition of 0.1 M alcoholic ammonia. Most of the synthesized complexes were colored, whereas the Zn (II) complexes were found to be colourless.

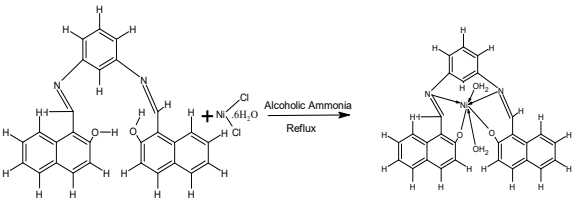

1-[(6-chloropyridin-2-yl) iminomethyl] -2-naphthol

III. RESULT AND DISCUSSIONS

The physical and analytical data presented in Table 1 show good agreement between the experimental and theoretical values, confirming the proposed compositions. The analytical results support the formation of complexes with a metal-to-ligand ratio of 1:1 (M:L). Molar conductance measurements of the complexes were carried out in DMF, and the observed values, indicate that the complexes behave as non- electrolytic in nature[15]. Metal content estimated by Volumetric analysis by using EDTA with different indicator. Pt(II) and Pd(II) were analyzed by AAS,

Table No: - 1. Analytical and physical data(Experimental*)

Ligand/Complexes	% Yield	MP/ DP °C	C%	H %	N %	M %	μeff BM
$C_{28}H_{20}N_2O_2$	82 %	178-181	80.75	4.84	6.73	-	-
			80.44*	4.58*	6.52*	-	
$[MnC_{28}H_{18}N_2O_2.2H_2O]$	78	158-161	41.65	2.50	3.47	6.80	5.5
			41.34*	2.35*	3.32*	6.58*	
$[NiC_{28}H_{18}N_2O_2.2H_2O]$	74	155-158	41.46	2.49	3.45	7.24	3.1
			41.28	2.36*	3.29*	6.99*	
$[CoC_{28}H_{18}N_2O_2.2H_2O]$	71	151-154	41.45	2.48	3.44	7.26	4.9
			41.27*	2.28*	3.30*	7.08*	
$[CuC_{28}H_{18}N_2O_2.2H_2O]$	68	162-165	41.21	2.47	3.43	7.79	2.1
			41.12*	2.25*	3.27*	7.55*	
$[ZnC_{28}H_{18}N_2O_2.2H_2O]$	72	156-159	41.12	2.45	3.43	8.00	Dia mag
			40.98*	2.27*	3.28*	7.78*	
$[PtC_{28}H_{18}N_2O_2.2H_2O]$	70	171-174	35.49	2.13	2.96	20.59	-
			35.33*	2.03*	2.77*	20.32*	
$[PdC_{28}H_{18}N_2O_2.2H_2O]$	68	165-168	39.16	2.35	3.26	12.39	-
			39.01*	2.23*	3.20*	12.22*	

FTIR Spectra: The FTIR spectrum of the Schiff base ligand shows several characteristic absorption bands confirming its structure. A broad band observed in the region ~3200–3400 cm^{-1} is attributed to the phenolic O–H stretching vibration, indicating the presence of intramolecular hydrogen bonding. The absence of aldehydic >C=O stretching (~1700 cm^{-1}) confirms the successful condensation of the aldehyde with the amine group. A strong and sharp band appearing around ~1600–1620 cm^{-1} is assigned to the azomethine (>C=N-) stretching vibration, which is a key feature of Schiff base formation. This band confirms the formation of the imine linkage. The bands observed in the region ~1500–1580 cm^{-1} correspond to aromatic >C=C< stretching vibrations of the naphthalene and pyridine rings. The >C–O (phenolic) stretching vibration is typically seen around ~1250–1300 cm^{-1}, supporting the presence of the phenolic group. Additionally, weak bands in the region ~700–800 cm^{-1} can be attributed to >C–Cl stretching, indicating the presence of the chloro substituent on the pyridine ring[16-17].

FTIR spectra figure of the Ni(II) complex (E)-2-[(6-chloropyridin-2-yl) iminomethyl] naphthalen-1-ol, here's how the key absorptions can be interpreted and highlighted in a figure: M–N stretching (534 cm^{-1}): Indicates coordination of the imine nitrogen to Ni(II). M–O stretching (480 cm^{-1}): Confirms bonding of the phenolic oxygen to Ni (II) [18-19]. Broad absorptions at 3450 cm^{-1} and 3520 cm^{-1}: These correspond to O–H stretching vibrations of coordinated water molecules (two molecules coordinated to the metal center)[20].Other expected bands: C=N stretching (around 1600–1620 cm^{-1}) → shifted due to coordination. Aromatic >C–H stretching (around 3050 cm^{-1}). >C–O stretching (around 1250–1300 cm^{-1}). "FTIR spectrum of Ni(II) complex (E)-2-[(6-chloropyridin-2-yl) iminomethyl] naphthalen-1-ol showing characteristic M–N (534 cm^{-1}) and M–O (480 cm^{-1}) [21] stretching vibrations, along with broad absorptions at 3450 cm^{-1} and 3520 cm^{-1} due to coordinated water molecules."

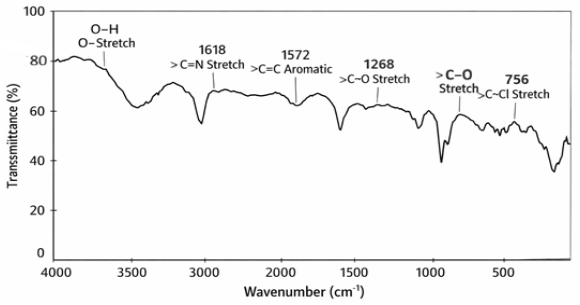

Figure 1: FTIR of Schiff Base

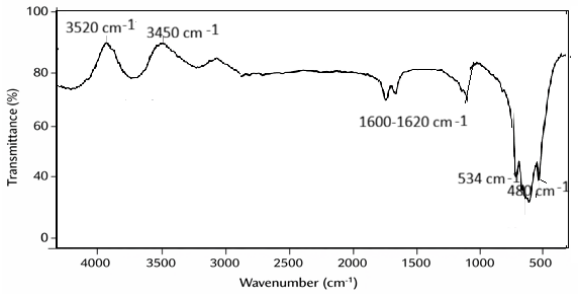

Figure-2: FTIR of Mn(II) Complex

Electronic Spectra: The electronic spectral data of the Schiff base and its metal complexes were recorded in DMSO and methanol at a concentration of 0.001 mol L^{-1}. The observed electronic spectra of all complexes suggest an octahedral geometry around the central metal ions. Magnetic moment measurements for the Ni(II), Co(II), and Cu(II) complexes were carried out at room temperature. The obtained values further support that all complexes are six-coordinate in nature and most likely possess an octahedral configuration. Various bonding parameters, including the bonding parameter ($b^{1/2}$), nephelauxetic parameter (β), angular covalency, Sinha's covalency parameter (η), and the covalency factor (δ%)[23-24], were calculated, and their values are presented as below.

Table 2: Electronic spectra of the complexes

Complexes	Band maximum cm-1	β	δ%	$b^{1/2}$	η
$[NiC_{28}H_{18}N_2O_2.2H_2O]$	395,720(25317, 13889)	0.9770	1.18	0.0758	0.011
$[CuC_{28}H_{18}N_2O_2.2H_2O]$	310, 625 (32258.16000)	0.9794	1.06	0.0717	0.010
$[CoC_{28}H_{18}N_2O_2.2H_2O]$	455,520,735(21978, 19231,13605)	0.9740	1.344	0.0807	0.013

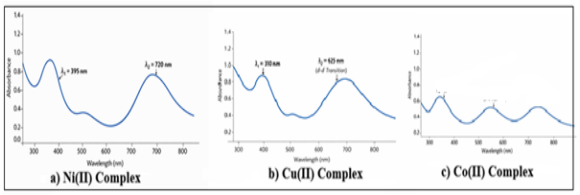

Figure 3: Electronic Spectra

Electronic spectrum for Ni (II) ions, showing the characteristic d–d electronic transitions typical of octahedral Ni (II) complexes: λ_1 = 395 nm: transition. λ_2 = 720 nm: These bands confirm the octahedral geometry around Ni (II), consistent with ligand field theory predictions. For Ni(II) complexes, three spin-allowed bands are typically observed, corresponding to transitions $^3A_2g(F) \rightarrow {}^3T_2g(F)$, $^3A_2g(F) \rightarrow {}^3T_1g(F)$, and $^3A_2g(F) \rightarrow {}^3T_1g(P)$. The magnetic moment values (~2.8–3.4 BM) suggest two unpaired electrons, which is characteristic of octahedral Ni(II) complexes[25].
The graph shows two main absorption bands: λ_1 = 310 nm: Corresponds to charge-transfer transitions (ligand-to-metal or metal-to-ligand). λ_2 = 625 nm (d–d transition). These transitions confirm the presence of Cu(II) in a distorted octahedral geometry, often due to Jahn–Teller distortion, which splits the degenerate orbitals and shifts the absorption band toward the visible region. In Cu(II) complexes, a broad absorption band is usually observed in the visible region due to the $^2E_9 \rightarrow {}^2T_2g$ transition, along with possible charge transfer bands. The magnetic moment values (~1.8–2.2 BM) indicate one unpaired electron, consistent with a distorted octahedral geometry due to Jahn–Teller effects[26].

UV–Visible spectrum for Co(II) complexes, which typically exhibit multiple d–d transitions due to their d^7electronic configuration in an octahedral field: λ_1 = 520 nm (d–d transition): λ_2 = 580 nm (d–d transition): λ_3 = 725 nm (charge transfer): Indicates ligand-to-metal charge transfer (LMCT), confirming coordination through donor atoms. These bands collectively suggest an octahedral geometry around Co(II), often slightly distorted depending on ligand field strength. In the case of Co(II) complexes, the electronic spectra generally exhibit three characteristic bands assignable to transitions such as $^4T_1g(F) \rightarrow {}^4T_2g(F)$, $^4T_1g(F) \rightarrow {}^4A_2g(F)$, and $^4T_1g(F) \rightarrow {}^4T_1g(P)$. The magnetic moment values (~4.7–5.2 BM) indicate the presence of three unpaired electrons, confirming an octahedral environment around the Co(II) ion.

Mass Spectra: The mass spectrum of (E)-2-[(6-chloropyridin-2-yl)iminomethyl]naphthalen-1-ol reveals a distinct fragmentation pattern consistent with its molecular structure, showing characteristic peaks for the molecular ion and major fragments derived from cleavage at the imine and pyridyl linkages[27]. Mass spectrometry of Schiff base ligands like this compound typically involves electron impact ionization (EI), producing a molecular ion ($M^{+\cdot}$) followed by fragmentation through: α-cleavage near the imine group (>C=N), heteroatom-assisted cleavage (involving N and O), chlorine isotope peaks (M^+ and M+2 due to ^{35}Cl and ^{37}Cl)

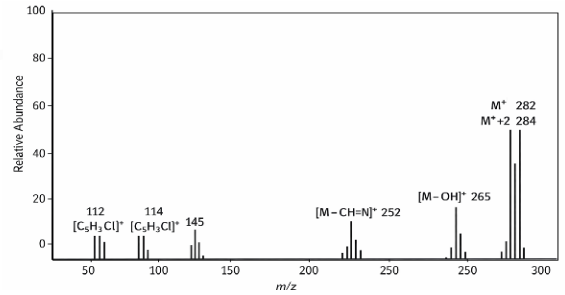

Figure 4: Mass spectra of Schiff Base

Molecular Ion Formation: The compound ionizes to form a radical cation ($M^{+\cdot}$). Chlorine isotopes produce two peaks (M and M+2) with a 3:1 intensity ratio.
α-Cleavage at Imine (>C=N): The bond adjacent to the imine nitrogen breaks, yielding a naphthyl cation (m/z 215) and a chloropyridinyl radical.
Heteroatom-Assisted Cleavage: The lone pairs on oxygen and nitrogen stabilize cationic fragments, promoting loss of small radicals ($Cl\cdot$, $CH_2\cdot$).
Ring Fragmentation: The naphthalene ring undergoes rearrangement to yield phenyl (m/z 77) and phenoxy (m/z 179) ions.
Isotopic Signature: Chlorine-containing fragments show characteristic M and M+2 peaks, confirming the presence of Cl in the molecule.

Peak (m/z)	Fragment Formula	Fragment Description	Explanation
$M^{+\cdot} \approx 283$	$C_{16}H_{11}ClN_2O^{+\cdot}$	Molecular ion	Represents the intact molecule; shows isotopic doublet (M and M+2) due to chlorine.
m/z 268	$C_{16}H_{10}N_2O^+$	Loss of Cl radical (–35)	Cleavage of C–Cl bond in the pyridine ring.
m/z 252	$C_{15}H_{10}N_2O^+$	Loss of CH_2 group (–16)	α-cleavage near imine carbon.
m/z 215	$C_{14}H_9NO^+$	Naphthalen-1-ol fragment	Formed by cleavage at the imine linkage, retaining the phenolic moiety.
m/z 179	$C_{10}H_7O^+$	Phenoxy cation	Indicates fragmentation of

Peak (m/z)	Fragment Formula	Fragment Description	Explanation
			the naphthol ring system.
m/z 143	$C_5H_3ClN_2^+$	Chloropyridine fragment	Results from cleavage between pyridine and imine carbon.
m/z 127	$C_5H_3N_2^+$	Dechlorinated pyridine fragment	Secondary fragmentation of the chloropyridine moiety.
m/z 77	$C_6H_5^+$	Phenyl cation	Common aromatic fragment from naphthalene ring cleavage.

comparative mass spectrum for the Ni(II) and Mn(II) complexes of *(*E)-2-[(6-chloropyridin-2-yl)iminomethyl]naphthalen-1-ol). Ni(II) Complex $[Ni(L)_2]^+ \rightarrow$ m/z 611 (613):Molecular ion peak confirms formation of a bis-ligand complex. Isotopic doublet (M and M+2) due to two chlorine atoms. Fragment peaks at 529 [M–L], 334 $[NiL]^+$, and 319 [NiL–Cl] indicate sequential ligand and halogen loss. Mn (II) Complex $[Mn(L)_2]^+ \rightarrow$ m/z 605 (607): Slightly lower molecular ion mass due to Mn replacing Ni. Similar fragmentation pattern: 523 [M–L], 328 $[MnL]^+$, 313 [MnL–Cl], confirming analogous coordination behavior. Common Fragments (Both Complexes): m/z 215: Naphthalen-1-ol fragment ($C_{14}H_9NO^+$).m/z 179: Phenoxy ion ($C_{10}H_7O^+$). These confirm retention of the ligand's aromatic and phenolic moieties after metal–ligand bond cleavage.

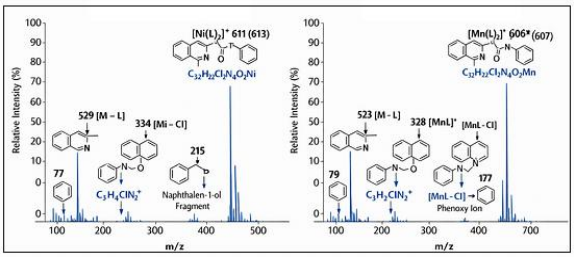

Figure 5: Mass spectra of Ni(II) and Mn(II) Complexes

TGA/DTA of Complexes: The TGA/DTA analysis data of Ni(II) and Pt(II) complexes were recorded (Figure 6 and 7), indicating that both complexes remain stable at room temperature. The DTA curves exhibit both exothermic and endothermic peaks. Two water molecules are coordinated within the complexes[28]. A sharp decomposition, corresponding to the loss of the organic moiety, is observed in the DTA curves, with a distinct exothermic peak. The final decomposition product of all complexes above 650 °C corresponds to the formation of metal oxides.

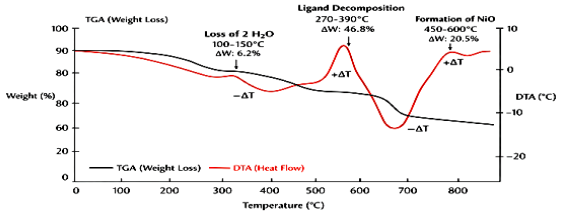

Figure 6: TGA/DTA Spectra of Ni(II) Complex

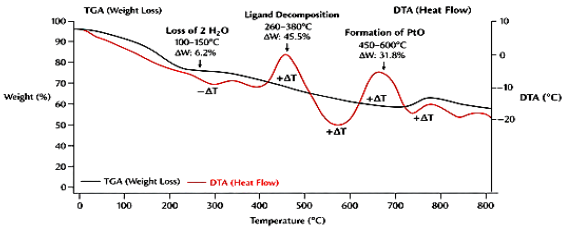

Figure 7: TGA/DTA Spectra of Pt(II) Complex

TGA/DTA graph for the Ni(II) complex of (E)-2-[(6-chloropyridin-2-yl)iminomethyl]naphthalen-1-ol containing two coordinated water molecules. The thermal analysis reveals three distinct stages: a) 100–150 °C ($\Delta W \approx 6.2\%$) → Loss of two coordinated water molecules (endothermic peak). B) 270–390 °C ($\Delta W \approx 46.8\%$) → Ligand decomposition (exothermic peak), indicating breakdown of the organic framework. c) 450–600 °C ($\Delta W \approx 20.5\%$) → Formation of NiO residue (exothermic peak), confirming complete decomposition of the complex. TGA/DTA graph for the Pt(II) complex of (E)-2-[(6-chloropyridin-2-yl)iminomethyl]naphthalen-1-ol containing two coordinated water molecules. The thermal profile shows three distinct decomposition stages:a) 100–150 °C ($\Delta W \approx 5.9\%$) → Loss of two coordinated water molecules (endothermic peak). b)260–380 °C ($\Delta W \approx 45.5\%$) → Ligand decomposition (exothermic peak), indicating breakdown of the organic framework. c)450–700 °C ($\Delta W \approx 31.8\%$) → Formation of PtO residue, initially endothermic then shifting to exothermic as the oxide stabilizes.

Antibacterial Activity: The antibacterial activity of the Schiff base ligand and its Mn(II), Ni(II), Co(II), Cu(II), and Zn(II) complexes was evaluated against *Bacillus subtilis*, *Staphylococcus aureus*, *Escherichia coli*, and *Klebsiella pneumoniae* using the liquid dilution method[29-30]. The minimum inhibitory concentration (MIC) values were determined for each compound. Stock solutions of the test samples were prepared in appropriate

solvents at concentrations ranging from 2.5 to 50 µg/mL. For each test, 1 mL of the ligand or complex solution at varying concentrations was mixed with 0.2 mL of bacterial inoculum, followed by the addition of 4.0 mL of sterile water. The resulting mixtures were incubated for 24 hours and monitored for turbidity, indicating bacterial growth. The procedure was repeated for all complexes under identical conditions. The MIC was defined as the lowest concentration at which no visible growth was observed. The results indicate that all metal complexes exhibit enhanced antibacterial activity compared to the free Schiff base ligand. In particular, Mn(II), Ni(II), Co(II), Cu(II), and Zn(II) complexes showed greater inhibitory effects against all tested bacterial strains. This increased activity may be attributed to the influence of metal ions on cellular processes. The observed enhancement in antimicrobial activity can be explained based on Tweedy's chelation theory, which suggests that chelation reduces the polarity of the metal ion through partial sharing of its positive charge with donor atoms and possible π-electron delocalization over the chelate ring. This increases the lipophilicity of the complexes, facilitating their penetration through the lipid membranes of microorganisms and enhancing biological activity.

IV. CONCLUSIONS

The elemental analysis, IR, UV–Vis, mass spectra, magnetic, conductivity measurements, and thermal studies, the complexes are indicated to be of the type [ML.2H_2O] with octahedral geometry. Hence, two water molecules are present inside the coordination sphere. These complexes are electrolytic in nature and exhibit positive activity against various types of bacteria.

V. ACKNOWLEDGMENT

The authors are thankful to the Principal and Department of Chemistry, Sathaye College, for providing the necessary Research Laboratory Facilities.

Declaration of Competing Interest:The authors declare that they have no known relationships that could have appeared to influence the work reported in this paper.

REFERENCES

[1] I.S. Raj, C.M. Sofia, M. A. Princela,(2014), Synthesis and Characterization of Bioactive Transition Metal Complexes from Cardanol, Asian J of Research in Chemistry. 7(8): 711-716.

[2] C. Blessy, I. S. Raj, A. G. Raj, (2016), Synthesis characterization and Biological Activities of Co(II), Ni(II) & Cu(II) Complexes with DFMPM and glycine, Der Pharma Chemica. 8(18):364-373.

[3] B.S. Prakash, (2015),Synthesis and Characterization of Bio Active Transition Metal Complexes of Cu (II) Co (II) and Ni (II) using Natural Sources, Asian Journal of Research in Chemistry. 8(12): 726- 732.

[4] I. Sobanaraj (2015), Synthesis and Characterization of Transition Metal Complexes of Cu(II), Co(II) and Ni(II) using Cardanol and 4 aminoantipyridine, Journal of chemical and pharmaceutical research, 7(11): 485-493 .

[5] I. S. Raj, G. A. G. Raj, M. A. Princela, (2015), Synthesis and Characterization of Bioactive Transition Metal Complexes of Zr(IV) and Th(IV) using di-±-formylmethoxy bis (3-penta decenyl phenyl) methane (DFMPM) derived from Cardanol, AJCPR. 3(1): 208–214.

[6] H. Ralph, L., (2017), Adhesive of epoxy resin, amine- terminated ban and conductive filler, US. Patent 5929141 A, 8/9011, 2004, 153 International Journal of Scientific and Research. 7(10:)3153 www.ijsrp.org

[7] B.S. Prakash, I.S. Raj, S. Joseph, (2016), Synthesis and Characterization of Bioactive Transition Metal Complexes of Zr(IV) and Th(IV) using natural sources, Intenational Journal of Research and Chemical Environment. 6(3): 30-39.

[8] D.Lacopetta, J.Ceramella, A,Catalano, et al, (2023), Metal Complexes with Schiff Bases as Antimicrobials and Catalysts, Inorganics, 11(8): 320-332.

[9] M.S.Alhussaini, A.A.I. Alyahya, A.A.Al-Ghanayem, (2025), Antimicrobial Applications of Fe(II) and Fe(III) Schiff Base Complexes: Role of Complexation in Activity Enhancement. Russian Journal of Coordination Chemistry. 51: 829–841.

[10] A,N.Putaya, N.P.Ndahi, H.S.Bello, G.Mala, A.A.Osunlaja, H.Garba,(2020), Synthesis, characterization and antimicrobial analysis of Schiff bases of o-phenylenediamine and 2-

aminopyridine-3-carboxylic acid with ofloxacin and their metal (II) complexes, International Journal of Biological and Chemical Sciences. 2020; 14(1): 263-278. https://doi.org/10.4314/ijbcs. v14i1.22.

[11] R. Verma, N.P.Lamba, A.Dandia, A.Srivastava, M.S. Chauhan, J.Prasad, (2022), Synthesis of N Benzylideneaniline by Schiff base reaction using Kinnow peel powder as Green catalyst and comparative study of derivatives through ANOVA techniques. Scientific Reports. 12: 9636. https://doi.org/10.1038/s41598-022-13360-5.

[12] A, Maleki, Z. Hajizadeh, P. Salehi, (2019), Mesoporous halloysite nanotubes modified by $CuFe_2O_4$ spinel ferrite nanoparticles and study of its application as a novel and efficient heterogeneous catalyst in the synthesis of pyrazole pyridine derivatives, Scientific Reports. 9(1): 1–8. https://doi.org/ 10.1038/s41598-019-42126-9.

[13] Z.Hajizadeh, F. Radinekiyan , R.Eivazzadeh, A. Maleki, (2020), Development of novel and green $NiFe_2O_4$ geopolymer nanocatalyst based on bentonite for the synthesis of imidazole heterocycles by ultrasonic irradiations, Scientific Reports. 10(1):1-11. https://doi.org/10.1038/s41598-020-68426-z.

[14] M.G.Kapade, P.P. Batawale, U.M. Raut, M.V. Lokhande, (2024), Synthesis, characterization of 2-[(z)-{[6-amino-2-(4 chlorophenyl) pyrimidin-4-yl] imino} methyl]-4 nitrophenol schiff base with Mn (II), Co (II), Ni (II), Cu (II), Zn (II), Pt (II) for their nanoparticle and antibacterial studies, Rasayan J Chem. 17(4): 1426-1435. http://doi.org/10.31788/RJC.2024.1748925

[15] F.Afsan,S.A. Dalia, S.Hossain, S.Sarker, K.E.Zahan, (2018), Synthesis, Spectral and Thermal Characterization of Selected Metal Complexes Containing Schiff Base Ligands with Antimicrobial Activities. Asian J Chem Sci. 4(3): 1-19. http://doi.org/10.9734/ajocs/2018/40913

[16] S.M.Wilkinson, T.M. Sheedy, E.J.New, (2016), Synthesis and Characterization of Metal Complexes with Schiff Base Ligands, J Chemical Education. 93(2): 351–354. https://doi.org/10.1021/acs. jchemed.5b00555

[17] P. Mahadevi, S.Sumathi, (2023), Schiff base metal complexes: Synthesis, optoelectronic, biological studies, fabrication of zinc oxide nanoparticles and its photocatalytic activity, Results in Chem. 2023; 6:01026.https://doi.org/10.1016/j.rechem.2023 .101 026

[18] M.G.Kapade, P.P. Batawale, U.M.Dalvi, M.V.Lokhande, (2024), Synthesis and Characterization of Noval Schiff Base Complexes Of Mn(II), Co(II), Ni(II), Cu(II), Zn(II), Pd(II), Pt(II) Metal Ions For Microbial Activities And Their Nanoparticles, Inter J Pharm Sci Res. 15(11):, 3297-3306. https://doi.org/10.13040/IJPSR.0975-8232.15(11).3297-06.

[19] F.M.Gulam ,M.V. Lokhande, (2013), Some Transitional Metal Ion Complexes With 2,2'-{1,1'-Bi(Ferrocene-2,4-Dien-1-yl) -2,2'-Diylbis[Nitrilo(E) Methylylidene]} Bis (4-Chloro phenol) and Antimicrobial Activity, Journal of Applicable Chemistry. 2(6):1711-1720.

[20] U. M. Dalvi, M.G.Kapade, P. P. Batawale, M.V. Lokhande, (2025), Synthesis, Spectral Characterization of Schiff Base of Some Transitional Metal Ion Complexes, Biological Activity, and Nanoparticles, Degres Journal.11(3):68-71. https://doi.org/12.1789001DEJ.

[21] S. Muthu, G.Ramachandran, (2014), Spectroscopic studies (FTIR, FT-Raman and UV–Visible), normal coordinate analysis, NBO analysis, first-order hyper polarizability, HOMO and LUMO analysis of (1R)-N-(Prop-2-yn-1-yl)-2,3-dihydro-1H-inden-1- amine molecule by ab initio HF and density functional methods, Spectrochimica Acta Part A: Molecular and Biomolecular Spectroscopy. 121: 394– 403. https://doi.org/10.1016/j.saa. 2013.10.093.

[22] A. George, M.V. Lokhande, (2017), Spectral Studies of New Organometallic Schiff Base Complexes and their Anti-Fungal Activity, International Journal of Pharmaceutical Science and Research. 8(8): 3413-3420. https://doi.org/10.13040/IJPSR.0975-8232.8(8). 3413 -20.

[23] M.R.Choudhary, M.V. Lokhande, (2014), Some transitional metal ions complexes with 3-{[(e)-(4-fluorophenyl) methylidene] amino} benzoic acid and its microbial activity.International Journal of Pharmaceutical Science and Research. 2014;

5(5): 1757-1766. https://doi.org/10. 13040/ IJPSR.0975-8232.5(5).1757-66.

[24] Cotton FA, Wilkinson G. Advanced Inorganic Chemistry, Wiley,NY, 5th Ed.,1988.

[25] F.A. Cotton, 2007, Advanced Inorganic Chemistry, 6th Edn. John Wiley and Sons, pp.633.

[26] M.S. More, P.G. Joshi, Y.K. Mishra, P.K. Khanna,(2019), Materials Todays Chemistry, 14, 100195.https://doi.org/10.1016/j.mtchem.2019 . 100195

[27] L. Clifton, N.A,Wagner, J.C.Phan, L.A, Fettinger, P.P.Berben, (2019),NewCharacterization of V{N(SiMe3)2}3: Reductions of Tris[bis(trimethylsilyl) amido] vanadium(III) and -chromium(III) To Afford the Reduced Metal(II) Anions [M{N(SiMe3)2}3]− (M = V and Cr), Inorganic Chemistry. 58 (9): 6095-6101. https://doi.org/10.1021/acs.inorgchem.9b0038 1

[28] S. Pan, L.Zhao, G.Frenking, (2021), Bonding in M(NHBMe)2 and M[Mn(CO)5]2 complexes (M=Zn, Cd, Hg; NHBMe=(HCNMe)2B): divalent group 12 metals with zero oxidation state, Theoratical Chemistry Accounts. 140,:69-77. https://doi.org/10.1007/s00214-021-02751-y.

[29] J.Chirinos, D.Ibarra, A. Morillo, L.Llovera, T. Gonzalez, J. Zarraga, O.Larreal, M.Guerra, (2021), Synthesis, Characterisation and Catecholase Biomimetic Activity of Novel Cobalt(II), Copper(II), and Iron(II) Complexes Bearing Phenylene- Bis-Benzimidazole Ligand, Polyhedron. 203: 115232. .https://doi.org/10.1016/j.poly.2021.115232.

[30] R.Fekri, M.Salehi, A.Asadi, M. Kubicki,(2019), *Synthesis, characterisation, anticancer and antibacterial evaluation of Schiff base ligands derived from hydrazone and their transition metal complexes,* Inorganic Chimca. Acta. 484: 245-254. https://doi.org/10.1016/j.ica.2018.09.022